Magnetic moment measurements in ^{86}Zr

A. W. Mountford, T. Vass, G. Kumbartzki, L. A. Bernstein, and N. Benczer-Koller
Department of Physics and Astronomy, Rutgers University, New Brunswick, New Jersey 08903

R. Tanczyn
Department of Physical Science, Kutztown University, Kutztown, Pennsylvania 19530

C. J. Lister, P. Chowdhury, and S. J. Freeman
A. W. Wright Nuclear Structure Laboratory, Yale University, New Haven, Connecticut 06511
(Received 4 October 1994)

The transient-field technique has been used to measure the g factors of yrast states in ^{86}Zr over the spin region $I = 8\hbar$–$14\hbar$ in order to ascertain the nature of the alignments at the first and second backbends. The states of interest were populated in the reaction ^{12}C(^{77}Se,3n) at 260 MeV. The results demonstrate that the first crossing at the 8^+_1 state involves the alignment of neutron $g_{9/2}$ quasiparticles, and that proton $g_{9/2}$ quasiparticles align at higher spin.

PACS number(s): 21.10.Ky, 27.50.+e

I. INTRODUCTION

Understanding the structure of transitional nuclei has proved to be extremely difficult. These nuclei lie far enough from shell closures to prohibit full microscopic calculations, and they have not developed sufficient collectivity to be reliably interpreted through deformed cranking models. The energies involved in single particle excitations, in collective vibrations and in collective rotations, are similar, so that states associated with each of these degrees of freedom tend to mix and thus have complicated wave functions with amplitudes from all three configurations. Understanding these mixing interactions, and how they evolve in the transitional regions spanning from collective to single particle structure, is the aim of this work.

Mass 80–90 nuclei are ideal for this type of research. Drastic changes of structure from deformed in the $N = Z$ nuclei to spherical near the $N = 50$ shell closure have been observed [1]. Zirconium isotopes ($Z = 40$) show some of the most dramatic changes, from the highly deformed ^{80}Zr to the ideal spherical nucleus ^{90}Zr. In the transition region, ^{84,86}Zr have been the focus of much recent attention. Aside from their transitional nature, these nuclei are easily polarized and are thus prime candidates for supporting superdeformation.

One framework for studying the mixing of different types of excitation is that of the extended interacting boson model (IBM-1) [2]. Here the collectivity (both vibrational and rotational) is described by the IBM, and single particle contributions can be incorporated through the coupling of unpaired fermions. This approach has been successful in interpreting bands in ^{84,86}Zr which have unusual properties [3]. One of the strengths of this model is the prediction of the transitional electromagnetic matrix elements which are quite irregular and difficult to reproduce through more conventional methods.

Recent work [4] on the transitional nucleus ^{86}Zr showed unusual band structures. At low spin, the $B(E2)$ values decrease with spin, a behavior inconsistent with either rotational or vibrational motion. At higher spin, the level spacings are characteristic of deformed rotational nuclei, but even and odd spin states are staggered in energy, a distribution that can be interpreted [4] as the signature-splitting associated with nonaxial shapes. Thus it appears that the nucleus has undergone a shape change favoring rotational motion. However, the evidence obtained from lifetime measurements is more complex. The $B(E2)$ values are small and $B(M1)$ values are large. This unusual behavior was interpreted within the framework of the extended IBM model incorporating two boson pairs. One of the questions not resolved by these measurements was the nature of the alignments in the yrast states. In this particular case, transitional matrix elements are not very sensitive to differentiating between proton or neutron alignments. However, static magnetic moments are sensitive to the type of aligning particles.

Evidence for g factor variation over two alignments has been presented previously for ^{238}Th [5]. Magnetic moments in the alignment region are dominated by quasiparticle contributions. The question open to experimental tests is whether the two quasiparticle aligned crossings in the A=80 region can be described by a *linear superposition* of aligned neutrons and protons rather than by neutrons or protons alone. In this region, the $g_{9/2}$ orbit is occupied by both valence neutrons and protons, leaving the possibility of significant neutron-proton interactions.

The exact nature of these states, particularly their proton or neutron parentage, can be identified more clearly if these measurements are augmented by the extraction of magnetic moments. Magnetic moments of aligned states can be written in terms of i, the aligned angular momentum contribution to the total spin I, g_R, the rotational value, and g_i, the g factor of the aligned nucleon, as [6]

$$\mu_I = g_R(I - i) + g_i i \ . \qquad (1)$$

The g factors of individual neutrons or protons in the $g_{9/2}$ orbit are given by the experimental values [7] $g_i^\nu = -0.24$ (from ^{87}Sr) or $g_i^\pi = +1.37$ (from ^{93}Nb). The measurement of magnetic moments in ^{84}Zr [8] has demonstrated that the particles that align at the lowest angular momentum in ^{84}Zr are protons rather than a superposition of aligned neutrons and protons.

In order to clarify whether the high-spin states in ^{86}Zr consist of four neutron, four proton, or mixed two proton-two neutron configurations, the g factors of the states, especially those for the 8^+ and 14^+ states need to be measured. A recent static field measurement [9] of the first isomeric ($\tau = 90$ ps) $I = 8\hbar$ state points to a structural change at low spin. In the present paper, measurements using the transient field technique of the magnetic moments of the short-lived higher spin yrast states in ^{86}Zr are described.

II. EXPERIMENTAL TECHNIQUE

The transient field technique, which was used in this experiment, has been successfully applied in this mass region on nuclei excited by HI-fusion evaporation reactions [8,10]. The experimental details for measuring magnetic moments of short-lived excited states by the transient field technique have been described in previous publications [11–13]; only details relevant to the current experiment are described here.

The reaction ^{12}C(^{77}Se,3n)^{86}Zr at 260 MeV was chosen to populate states in the region where four quasiparticle alignment occurs ($I = 14\hbar$), because it yielded the highest production cross section for ^{86}Zr. At this beam energy, only states up to about 6.9 MeV were excited, limiting the deexcitation paths into the lower levels of the nucleus, and allowing side feeding patterns to be taken into account explicitly in the analysis. This emphasis on the higher spin states was, however, detrimental to the measurements at lower spin, as the observed precessions of the γ–ray angular distributions reflect the entire deexcitation process. A partial level scheme showing the states populated in the experiment is given in Fig. 1.

The target was prepared by dipping a copper-backed (5.74 mg/cm^2) iron foil (6.78 mg/cm^2) in a carbon suspension. A thin C film, 0.41 mg/cm^2 thick, was thus deposited on both faces of the substrate. The average entrance and exit energies and velocities for the Zr ions in the iron layer were 202.7 MeV, $9.7v_0$ and 11.5 MeV, $2.3v_0$ respectively. $v_0 = e^2/\hbar$ is the Bohr velocity. The average transit time through the iron layer was 0.73 ps. The magnetization of the target was measured at 0.1748 T.

Four Compton-suppressed Ge detectors (~20%) were placed at nominal angles of ± 56° and ± 124° with respect to the beam direction and at a distance of 18.2 cm from the target. A 12.5 cm × 12.5 cm, NE213 neutron detector was located downstream at 0° at a distance of 14 cm from the target. Pulse shape discrimination and neutron time-of-flight techniques were used for γ-ray suppression.

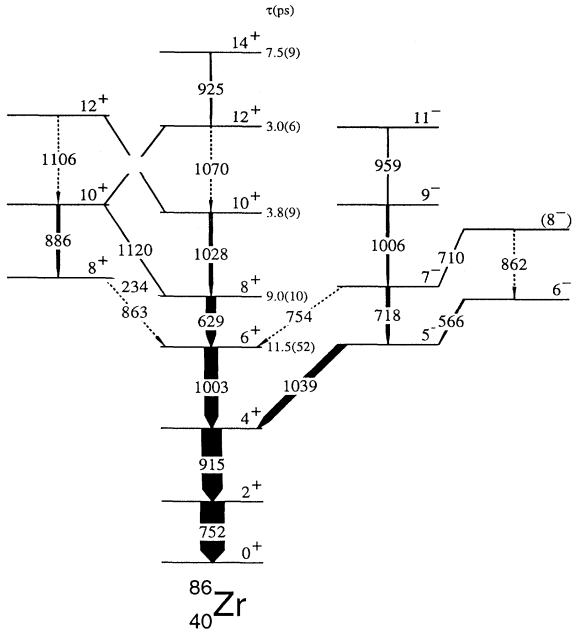

FIG. 1. ^{86}Zr energy levels observed in the ^{12}C(^{77}Se,3n)^{86}Zr reaction at 260 MeV. Transition energies are in keV. The transitions indicated by dotted lines were either doublets, contaminations or very weakly observed.

The data were recorded in event mode and both n-γ coincidences and single γ-ray yields were recorded. Angular distributions $W(\theta)$ were measured in both singles and coincidence modes with two γ-ray detectors, one acting as a monitor and one being moved through angles of interest.

In addition, a specific measurement of the logarithmic slope, $S(\theta_0) = (1/W)(dW/d\theta)$, of the angular distribution at the angle $\theta_0 = 56°$ was carried out during the precession runs by relocating the four γ-ray detectors every two hours from 58° and 126° to 54° and 122°. The logarithmic slopes of the angular distributions obtained by both methods were in agreement. The average experimental logarithmic slopes $S_{\rm expt}$ obtained from these two measurements are shown in Table I.

The measured effect ϵ^n for the radiation deexciting the state n can be expressed as

$$\epsilon^n(\theta_0) = \frac{\rho^n - 1}{\rho^n + 1}, \qquad (2)$$

where $\rho^n = (\rho^n_{14}/\rho^n_{23})^{1/2}$ is determined from the double ratios

$$\rho^n_{ij} = \sqrt{\frac{N_i^{\uparrow n}/N_i^{\downarrow n}}{N_j^{\uparrow n}/N_j^{\downarrow n}}}, \qquad (3)$$

and the coefficients $i = 1, 2$, $j = 3, 4$ represent the four detectors; $N_{i,j}^{\uparrow n}$ and $N_{i,j}^{\downarrow n}$ are the coincidence or single counting rates of the photopeak of the transition $I_n \rightarrow I_{n-1}$ in the ith or jth detector with the external field

TABLE I. γ-ray energies, intensities, experimental and model logarithmic slopes S, observed effects, and precession angles $\Delta\theta$ derived for the given transitions in ^{86}Zr.

$J_i^\pi \rightarrow J_f^\pi$	E_γ (keV)	I_γ	$S(56°)_{\text{expt}}$	$S(56°)_{\text{model}}$	$\epsilon(\times 10^{-3})$	$-\Delta\theta$ (mrad)	g
$2_1^+ \rightarrow 0_1^+$	752	100	−0.25(7)	−0.29(3)	11.86(102)	41.2(53)	
$4_1^+ \rightarrow 2_1^+$	915	83	−0.32(8)	−0.29(3)	14.35(125)	49.8(65)	
$6_1^+ \rightarrow 4_1^+$	1003	55	−0.33(9)	−0.32(1)	15.16(146)	47.2(47)	
$8_1^+ \rightarrow 6_1^+$	629	40	−0.35(136)	−0.32(1)	12.84(275)[b]	40.0(86)	−1.05(64)
$10_1^+ \rightarrow 8_1^+$	1028	14	−0.25(26)	−0.33(5)	6.04(428)	18.5(133)	−0.48(96)
$12_1^+ \rightarrow 10_1^+$	1070	9[a]	−0.34(15)	−0.33(5)	14.14(624)[b]	43.2(200)	−0.35(85)
$14_1^+ \rightarrow 12_1^+$	925	4	−0.25(184)	−0.33(5)	36.5(102)	111(35)	1.86(61)
$8_2^+ \rightarrow 8_1^+$	234	16	−0.13(17)	−0.13(4)	16.85(353)[b]	131(46)	1.06(22)[c]
$10_2^+ \rightarrow 8_2^+$	886	12	−0.46(27)	−0.35(3)	21.62(502)	62(15)	
$12_2^+ \rightarrow 10_2^+$	1106	6[a]	−0.34(13)	−0.36(6)	12.97(214)	35.8(86)	0.55(13)
$5^- \rightarrow 4^+$	1039	29	+0.21(13)	+0.15(5)	−3.82(228)	26(18)	
$7^- \rightarrow 5^-$	718	14	−0.04(29)	−0.21(6)	4.21(519)[b]	20(26)	0.46(21)[d]
$9^- \rightarrow 7^-$	1006	8	−0.20(29)	−0.22(7)	13.72(597)	62(34)	

[a]These lines were contaminated by other unresolved transitions of almost the same energy. An estimate of their intensity was made for the analysis.
[b]Results obtained from the n-γ coincidence experiment.
[c]Average value for the 8_2^+ and 10_2^+ states.
[d]Average value for the 5^-, 7^-, and 9^- states.

up(↑) or down(↓) with respect to the plane of the reaction corrected for random and/or background rates. Similar "cross ratios," $\rho_c^n = (\rho_{24}^n/\rho_{13}^n)^{1/2}$ and ϵ_c^n, were calculated from the data in order to check for systematic effects that might mask the true precession. In all cases, vanishingly small ϵ_c^n were obtained.

III. ANALYSIS AND RESULTS

The double ratios ρ obtained from the γ-ray single spectra were found to be in good agreement with those obtained from the neutron-coincidence spectra. Since the statistics in the singles data were significantly superior, the data from the singles spectra were predominantly used for the analysis, except where there were obvious contaminants in the spectra. For example, the $8_1^+ \rightarrow 6_1^+$ (629 keV) transition was heavily contaminated with an activity line from ^{86}Sr. A typical γ-ray single spectrum is shown in Fig. 2.

Since the experimental values of $S(\theta)$ must be consistent with the observed feeding pattern, a set of "model" logarithmic slopes $S(\theta)_{\text{model}}$, based on the observed level scheme, was calculated which best fitted all experimental angular distribution data simultaneously. The precession angles $\Delta\theta = \epsilon/S_{\text{model}}$ for the states of interest were then

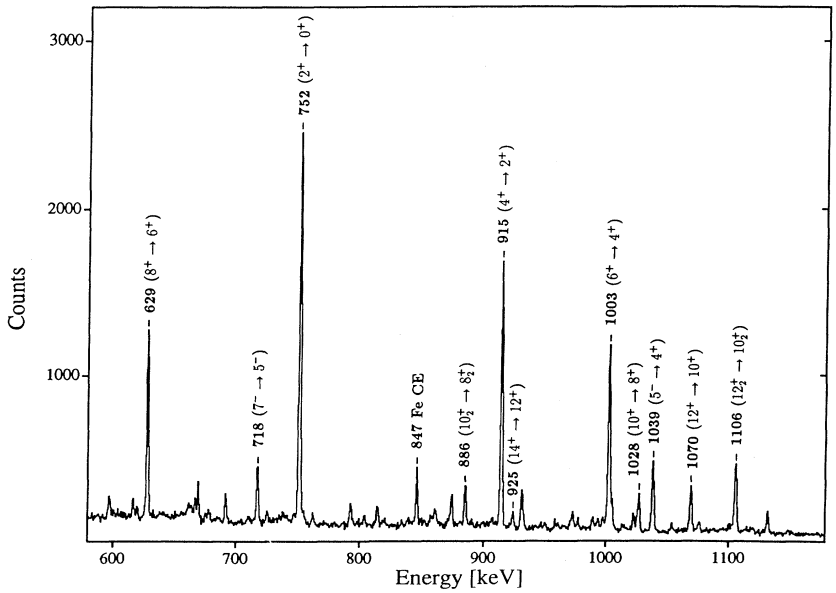

FIG. 2. γ-ray "singles" spectrum for ^{86}Zr from the ^{12}C(^{77}Se,3n)^{86}Zr reaction at 260 MeV. The γ-ray energies are in keV. The line at 847 keV corresponds to the $2_1^+ \rightarrow 0_1^+$ transition in Coulomb-excited ^{56}Fe.

obtained from the measured ϵ's, the logarithmic slopes of the angular distributions, and the known feeding intensities. The g factors were derived from these data through a complex procedure developed in a number of previous publications [8,10,13], which applies specifically to nuclei excited in (HI,xn) reactions.

The $S(\theta)_{\rm model}$ values were obtained by varying the initial degree of alignment produced in the reaction and calculating the subsequent loss of alignment as the nucleus decayed to the ground state. The A_4 coefficient of the angular distribution was linked to the A_2 coefficient via the alignment-yrast curve described by Zobel [14]. Additional loss of alignment from discrete feeding was considered explicitly. The final model values for the logarithmic slopes, corresponding to $\chi^2_{\rm min}$, are shown in Table I. The errors in the slopes were determined from the values of the A_2 and A_4 coefficients obtained for $\chi^2 = \chi^2_{\rm min} + 1$.

The total precession accumulated by each state is determined by the g factor of the state of interest, and by the precessions accumulated by the preceding states in the cascade. An analysis procedure similar to that used in previous work in this region [8,10] was followed. A computer code was written which followed the time evolution of the nucleus as it slowed down in the iron foil. The Rutgers [11] transient field parametrization was used,

$$B_{\rm TF}(v) = 96.7 \left(\frac{v}{v_0}\right)^{0.45} Z^{1.1} M, \qquad (4)$$

where M is the iron foil magnetization. Following its emergence from the ferromagnet, the nucleus was allowed to complete its decay in the perturbation free environment of the copper backing. It is worth noting that in this experiment, the lifetimes of all the states considered are longer than the transit time of the recoils through the target (0.73 ps) and the stopping time in the backing. Thus, the resulting precessions shown in Table I correspond to states that have experienced the full transient field; no Doppler broadenings of the γ-ray lines were observed.

The g factors listed in Table I were extracted directly from the experimental rotations assuming the feeding and decay history for the yrast states shown in Fig. 1, and the transient hyperfine field experienced during the recoil slow-down. Here the lifetimes were taken from previous work [15,16]. The side-feeding times were assumed to be 0.1 ps, which seems to be a reasonable upper limit on the basis of previous lifetime measurements in this mass region [8,10]. The results are not sensitive to variations in the feeding lifetimes. The g factor of the feeding continuum states was taken to be $g_c = 0.5$ [8,10]. The stopping powers used in the analysis were taken from Ref. [17]. The errors on the final g factors are large due to the covariance in the analytical procedure. The g factors for the lower lying states could not be extracted due to the long lifetime ($\tau = 90$ ps) of the 8^+_1 state, which forces the precessions of the low-spin states to reflect feeding only and not be sensitive to their own g factors.

The g factors predicted by the model for four different modes of particle excitation are plotted in Fig. 3(a).

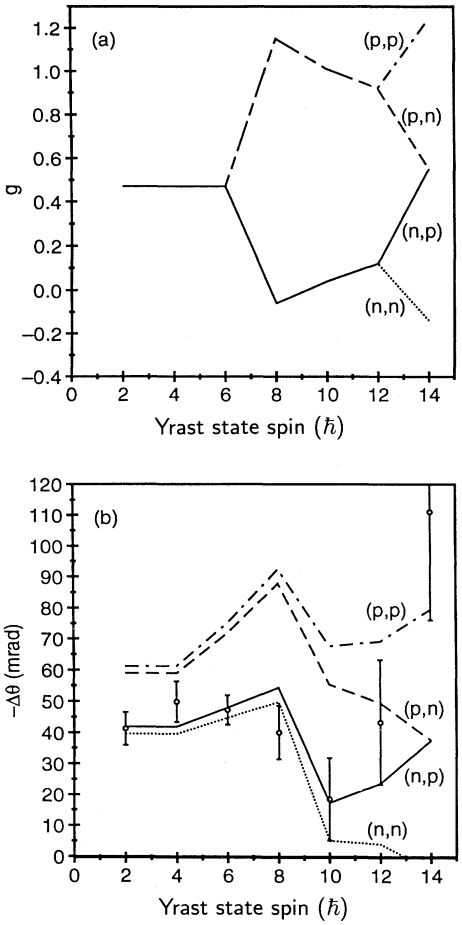

FIG. 3. (a) The g factors of yrast band states calculated using Eq. (1) for four scenarios: solid line (—), neutron followed by proton alignment; dotted line (· · ·), neutron followed by neutron alignment; dot-dashed line (· – ·–), proton followed by proton alignment; dashed line (– –), proton followed by neutron alignment. A gain of $6\hbar$ alignment at each crossing has been assumed. (b) The experimental precession angles for yrast states (open circles) compared with the values calculated with the g factors of Fig. 3(a), side-feeding lifetimes of 0.1 ps, a continuum g factor $g_c = 0.5$, and the decay scheme parameters shown in Fig. 1.

The predicted final rotations are plotted in Fig. 3(b), and are contrasted with the observed experimental precessions. The g factors used for these calculations correspond to the four possible combinations where the first and second alignments are attributed to either protons or neutrons. The alignment is assumed to occur suddenly at each crossing and to contribute $6\hbar$ of aligned angular momentum.

IV. DISCUSSION

The low-lying states in ^{86}Zr are almost equally spaced and exhibit decreasing $B(E2{:}\ I \rightarrow I\text{-}2)$ values, the $2^+_1 \rightarrow$

0_1^+, $4_1^+ \rightarrow 2_1^+$, $6_1^+ \rightarrow 4_1^+$ transitions being only 13.8(23), 6.3(28), and 3.0(13) W.u. [16], respectively. These facts alone imply that no simple collective model is appropriate. The level spacings indicate anharmonic vibration, but if that were the case, increasing $B(E2)$ values would be expected. The observed features are more easily explained in microscopic models where the decrease in collectivity reflects the limited number of configurations at low spin.

Three spin $I = 8\hbar$ states are anticipated (and observed both in this nucleus and in the neighboring strontium isotone). One is related to the collective $2_1^+ \rightarrow 4_1^+ \rightarrow 6_1^+$ sequence and has a complex wave function consisting of a mix of many configurations, while the other two have rather pure configurations corresponding to a pair of neutrons or protons in the $g_{9/2}$ shell which decouples and aligns to maximum spin. The relative positions of these states reveal a great deal about the positions of single particle levels relative to the Fermi surface. These features in turn are related to the shape and softness of the core potential in which the nucleons move. For example, a study of the krypton isotopes [18] shows that in a deformed shell model potential with prolate deformation, the proton decoupling and alignment is observed first, while for an oblate potential with similar deformation, the neutron alignment occurs earlier. In both these cases the collective rotational state lies slightly above the first alignment. In a truncated spherical shell model, the neutron alignment is lowest, followed by that of the protons, with the "collective" state at higher excitation. Studies of strontium and krypton isotopes [10,19] have shown that g factor measurements provide the only definitive way to experimentally reveal the structure of the $I = 8\hbar$ state and infer the shape of the nuclear potential.

The current data on the 8_1^+ state together with the static field measurement [9] indicate that the g factor falls below the collective value of 0.47, and is even negative. This result clearly suggests neutron alignment and that the nucleus is not prolate. The 8_2^+ and 10_2^+ states have precessions consistent with g factors larger than the collective value. The statistics on the measurements for these states are poorer than those for the yrast states. Nevertheless, an average g factor, $\langle g(8_2^+, 10_2^+)\rangle = 1.06(22)$ was obtained. A g factor, $g = 0.55(13)$, was also obtained for the 12_2^+ state, although the observed γ line was contaminated by other unresolved transitions. These data are consistent with a proton alignment description and indicate a slightly oblate or even spherical shape. A candidate for the 8_3^+ state at 3.79 MeV has been reported, but is unfortunately sufficiently nonyrast that it was not observed in this work.

Above 5.3 MeV and $I = 12\hbar$, there is sufficient energy available for two pairs of particles to decouple and align to form states of even higher spin. Here four sets of states are anticipated: a "collective" set, plus three sets of states each with four quasiparticles — all neutrons, all protons, or mixed neutrons and protons. Only one of these bands is known from experiment [4]. The observed band has small $B(E2)$ values, but alternating large and small $B(M1)$ transitions. It is of considerable interest to identify which of these bands is the one seen in experiment, as this fact would reveal if the potential is evolving in shape with angular momentum.

In the IBM + quasiparticles model, the "all neutron" band is anticipated to lie lowest, further reflecting the lower position of the first neutron alignment. Both four quasiprotons and four quasineutrons are calculated to reproduce the pattern of transitional matrix elements which have been measured. Unfortunately, the properties of the mixed proton-neutron configuration are beyond the scope of the first (IBM-1 core) version of the model, so its position and properties have not been calculated. The mixed configuration is the one predicted lowest in deformed shell model calculations, but in this latter framework it is difficult to reproduce the energy spacings.

Our g factor measurements at the highest spins show a swing from negative to positive values. This effect can only arise from proton contributions to the wave function. The value of $g = +1.86(61)$ clearly rules out a pure four quasineutron scenario, as well as the "collective" state. Two possibilities remain: the four aligned proton scenario, or that due to mixed neutron-proton configurations. To bring the proton single particle states lower than the neutron ones requires deformation of the potential to a prolate shape, which would result in considerable enhancement of the $B(E2)$ matrix elements in contradiction to the data. Thus, the mixed proton-neutron scenario with modest (or no) static deformation of the potential to the highest spin seems most likely.

Finally a comment on the negative parity states. Their precessions reveal positive g factors, and thus mainly proton aligned configurations such as $(g_{9/2}, p_{3/2})$. However, the measured average value of $\langle g(5^-, 7^-, 9^-)\rangle = +0.46(21)$ is much lower than that expected for a pure single particle aligned configuration, $g = +1.4$ [7]. Thus it may well be that, in the negative parity states, mixing of neutron and proton aligned configurations occur.

In conclusion, g factors up to spin $I = 14\hbar$ have been measured in the ^{86}Zr nucleus. The combination of static and transitional matrix elements help clarify structural assignments. The highest spin states have positive g factors, and the previously suggested pure neutron alignment can be excluded. The data were useful in confirming the nature of the low spin alignments. The further extension of microscopic models, both larger shell models and more generalized boson-fermion approaches, remains vital for studying the mechanism for the mixing of configurations and the evolution of collective behavior in transitional nuclei.

ACKNOWLEDGMENTS

The authors wish to thank Mr. A. Lipski for helping with the target preparation. We also are thankful to the staff of the Wright Nuclear Structure Laboratory for their accelerator support. This work was supported in part by the National Science Foundation and the Department of Energy.

[1] R. Bengtsson, in *Proceedings of the International Workshop on Nuclear Structure of the Zirconium Region, Bad Honnef, West Germany, 1988,* Research Reports in Physics, edited by J. Eberth, R.A. Meyer, and K. Sistemich (Springer-Verlag, New York, 1988).
[2] F. Iachello and D. Vretenar, Phys. Rev. C **43**, R945 (1991).
[3] A.A. Chishti, P. Chowdhury, D.J. Blumenthal, P.J. Ennis, C.J. Lister, Ch. Winter, D. Vretenar, G. Bonsignori, and M. Savoia, Phys. Rev. C **48**, 2607 (1993).
[4] P. Chowdhury, C.J. Lister, D. Vretenar, Ch. Winter, V.P. Janzen, H.R. Andrews, D.J. Blumenthal, B. Crowell, T. Drake, P.J. Ennis, A. Galindo-Uribarri, D. Horn, J.K. Johansson, A. Omar, S. Pilotte, D. Prévost, D. Radford, J.C. Waddington, and D. Ward, Phys. Rev. Lett. **67**, 2950 (1991).
[5] O. Häusser, H. Gräf, L. Grodzins, E. Jaeschke, V. Metag, D. Habs, D. Pelte, H. Emling, E. Grosse, R. Kulessa, D. Schwalm, R.S. Simon, and J. Keinonen, Phys. Rev. Lett. **48**, 383 (1982).
[6] S. Frauendorf, Phys. Scr. **24**, 349 (1981).
[7] P. Raghavan, At. Data Nucl. Data Tables **42**, 189 (1989).
[8] A.W. Mountford, J. Billowes, W. Gelletly, H.G. Price, and D.D. Warner, Phys. Lett. B **279**, 228 (1992).
[9] M. Weisflog, C.J. Gross, A. Harder, M.K. Kabadiyski, K.P. Lieb, A. Raguse, D. Rudolph, J. Billowes, T. Burkardt, J. Eberth, T. Myläus, and S. Skoda, Manchester University, Annual Report, 1993.
[10] A.I. Kucharska, J. Billowes, and C.J. Lister, J. Phys. G **15**, 1039 (1989).
[11] N.K.B. Shu, D. Melnik, J.M Brennan, W. Semmler, and N. Benczer-Koller, Phys. Rev. C **21**, 1828 (1980).
[12] N. Benczer-Koller, M. Hass, and J. Sak, Ann. Rev. Nucl. Sci. **30**, 53 (1980).
[13] A.W. Mountford, Ph.D. thesis, University of Manchester, 1992.
[14] V. Zobel, L. Cleeman, J. Eberth, H.P. Hellmeister, W. Neumann, and N. Wiehl, Nucl. Instrum. Methods **171**, 223 (1980).
[15] E.K. Warburton, C.J. Lister, J.W. Olness, P.E. Haustein, S.K. Saha, D.E. Alburger, J.A. Becker, R.A. Dewberry, and R.A. Naumann, Phys. Rev. C **31**, 1211 (1985).
[16] M. Avrigeanu, V. Avrigeanu, D. Bucurescu, G. Constantinescu, M. Ivascu, D. Pantelica, M. Tanase, and N.V. Zamfir, J. Phys. G **4**, 261 (1978).
[17] J.F. Ziegler *et al.*, *The Stopping and Range of Ions in Solids* (Pergamon, New York, 1985).
[18] C.J. Gross, J. Heese, K.P. Lieb, S. Ulbig, W. Nazarewicz, C.J. Lister, B.J. Varley, J. Billowes, A.A. Chishti, J.H. McNeill, and W. Gelletly, Nucl. Phys. **A501**, 367 (1989).
[19] J. Billowes, F. Cristancho, H. Grawe, C.J. Gross, J. Heese, A.W. Mountford, and M. Weiszflog, Phys. Rev. C **47**, R917 (1993).